# Ground state spin and excitation energies in half-filled Lieb lattices

M. Ţolea and M. Niţă*
*National Institute of Materials Physics, P.O. Box MG-7, 77125 Bucharest-Magurele, Romania*
(Received 17 March 2016; revised manuscript received 30 August 2016; published 3 October 2016)

We present detailed spectral calculations for small Lieb lattices having up to $N = 4$ number of cells, in the regime of half-filling, an instance of particular relevance for the nanomagnetism of discrete systems such as quantum dot arrays, due to the degenerate levels at midspectrum. While for the Hubbard interaction model—and even number of sites—the ground state spin is given by the Lieb theorem, the inclusion of long-range interaction—or odd number of sites—makes the spin state not known *a priori*, which justifies our approach. We calculate also the excitation energies, which are of experimental importance, and find significant variation induced by the interaction potential. One obtains insights on the mechanisms involved that impose as ground state the Lieb state with lower spin rather than the Hund one with maximum spin for the degenerate levels, showing this in the first and second orders of the interaction potential for the smaller lattices. The analytical results agree with the numerical ones, which are performed by exact diagonalization calculations or by a combined mean-field and configuration interaction method. While the Lieb state is always lower in energy than the Hund state, for strong long-range interaction, when possible, another minimal spin state is imposed as ground state.

DOI: 10.1103/PhysRevB.94.165103

## I. INTRODUCTION

The side-centered square lattice, i.e., the Lieb lattice, was first proposed in Ref. [1] as a rigorous example of itinerant ferromagnetism in the presence of on-site Hubbard interactions at half-filling. Recently, the Lieb lattice received renewed attention in the context of optical and photonic lattices [2–7], two-dimensional (2D) superconductivity [8,9], and for its specific topological properties [10–15]. In particular, the artificial lattice realization offers the advantage of controlling parameters, leading to various regimes not available in real-atom lattices, so that one can test a vast spectrum of theoretical predictions.

The Lieb lattice can have nontrivial magnetic properties [16–23] and its own specificity originates in the degenerate energy level, called also a flat band (see, e.g., Refs. [1,24–26]), which is located at the middle of the spectrum. This flat band is one from the total of *three* bands of the Lieb lattice, consistent with the three-atom unit cell. While the electron-hole symmetry imposes that this band is located at precisely *zero* energy, its exact degeneracy for a given finite lattice depends also on the border conditions.

Let us now picture a situation in which such a flat band is half-filled. Then, a legitimate question would be whether the system obeys the Hund rule with maximum spin of the electrons on the degenerate levels, say $s = s_{\max}$, or whether they have a lower total spin. The applicability of the Hund rule in various nanosystems has been a subject of considerable interest (see, e.g., Refs. [27–36]), both from applicative and fundamental points of view, for understanding the most intimate mechanisms of magnetism. The results presented in this paper shall add to the existing debate an instance when the Hund rule does not apply.

At this point it is important to mention two well-known theorems that give the ground state spin for some particular lattices with Hubbard interaction. We shall also define some labeling of states used in the paper:

(1) The Lieb theorem [1] states that, for a half-filled bipartite lattice (composed of two sublattices, say, A and B, and with hopping only between sites from different sublattices), with even total number of sites and with on-site Hubbard repulsion, the spin of the ground state is $s_L = \frac{1}{2}||A| - |B||$ ($|A|$, being the number of sites of the sublattice A). Needless to say, the Lieb lattice itself is bipartite. Its ground-state spin is thus given by the site number mismatch between the two sublattices, with the theorem stating also that the ground state is not degenerate (excluding the trivial $2s_L + 1$ spin degeneracy). The state lowest in energy from the subspace with spin $s_L$ shall be referred throughout the paper as the Lieb state.

(2) The Mielke theorem [24] states that a flat band located at the lowest part of the spectrum will always have the maximum spin ground state $s_{\max}$, if filled up to at most half, in the presence of Hubbard interaction. For exactly half-filling, the maximum spin ground state may be degenerate only with the state with a single spin flipped (excluding again the trivial spin degeneracy). Throughout this paper, such a state with the maximum spin value of the electrons in a flat band or degenerate level will be referred as a Hund state with spin $s_H = s_{\max}$, for the correspondence with the atomic physics rule.

In this paper we shall address finite Lieb lattices with up to $N = 4$ number of cells, or elementary squares, as the one depicted in Fig. 1, and we shall impose vanishing boundary conditions. Technically, this means that we can start from the infinite two-dimensional (2D) Lieb lattice from which one cuts the smaller lattice of interest by imposing the wave functions to be *zero* on the exterior points (for the square in Fig. 1 the wave functions vanish on the sites $B_{21}$, $B_{22}$, $C_{12}$, etc., that are not drawn), as opposed to periodicity conditions. The vanishing boundary conditions are particularly relevant for small lattices, with influence on the physical properties. In Ref. [16], for instance, the authors consider antiperiodic conditions instead, and obtain a different number of levels in the flat band.

For our case, the midspectrum level degeneracy is $g = N + 1$ [15] and the interesting problem here is that the spin values predicted by the above theorems at half-filling are different. They are $s_L = (N - 1)/2$ for the Lieb state and

*nitza@infim.ro

 

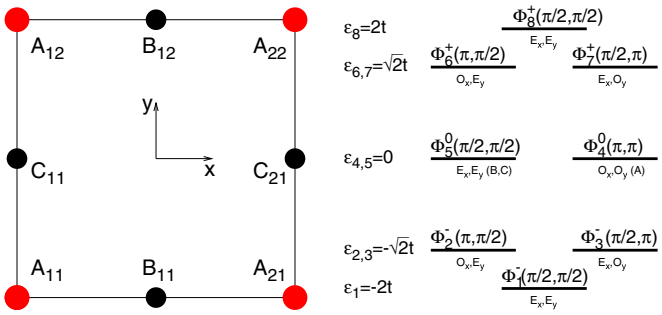


FIG. 1. (Left) The one-cell Lieb lattice with eight sites. The indices $n$, $m$ of the atoms $A$, $B$, and $C$ count the three-sites cells. (Right) The single-particle eigenstates $\Phi_\alpha(k_x,k_y)$ and eigenvalues $\epsilon_\alpha$ with $\alpha = 1,\ldots,8$. There are three sets of eigenstates: $\Phi^+$ for $\epsilon > 0$, the midspectrum degenerate levels $\Phi^0$ for $\epsilon = 0$ (called also flat band), and $\Phi^-$ for $\epsilon < 0$. The states marked with $E_x$ and $E_y$ are the states with even parity on $x$ and $y$ axes respectively and the states marked with $O_x$ and $O_y$ have odd parity. The two states in the flat band are nonoverlapping, being localized on different lattice points, $\Phi^0_4$ on $A$ sites $[\Phi^0_4(A) \neq 0, \Phi^0_4(B,C) = 0]$ and $\Phi^0_5$ on $B,C$ sites $[\Phi^0_5(A) = 0$ and $\Phi^0_5(B,C) \neq 0]$.

$s_H = (N+1)/2$ for the Hund one [37], being related by the formula $s_L = s_H - 1$ and suggesting a single spin-flip process between them. However, as shall be shown, one does not face a contradiction since the Lieb lattices do not have the degenerate flat band at the bottom of the spectrum but in its middle, and we shall show that the interaction with the below electrons proves decisive in imposing the ground state spin. Nevertheless, it shall be insightful throughout the paper to discuss also the spin properties of the *isolated* degenerate levels for small Lieb lattices; hence the relevance of the Mielke theorem here.

Both the Lieb and Mielke theorems have been rigourously proven only for on-site Hubbard interaction, so if one includes as well long-range interaction, the results are no longer known *a priori*, justifying our approach. Also, for the case of nanosystems, one is typically interested not as much in the ground states configurations, but especially in the excitation energies, which are the experimentally measurable quantities. Moreover, we shall give insights on the mechanisms that impose the Lieb state as the ground state using the nonoverlapping property of one of the states in the midspectrum [15] and the electron-hole symmetry of the Hamiltonian [38–40].

In this paper, particular attention will be paid to the smallest one-cell Lieb lattice depicted in Fig. 1, which allows (having only eight sites) an analytical solution at small interactions, as well as numerical exact diagonalization for any value of the interactions. If only Hubbard interaction is considered, we are in the frame of the Lieb theorem. However, our alternative proof for this specific system allows for an insight on the role of the states' spacial distributions and their symmetry properties. Similar arguments are presented for a two-cell Lieb lattice that, having odd number of sites, falls outside of the Lieb theorem conditions. The long-range interaction included in our calculations will show that the ground state spin remains unaffected, even if the electronic configuration itself may change.

For lattices of sizes $N = 2 \div 4$, numerical results will be presented by making use of a combined mean-field and configuration-interaction method (see, e.g., Refs. [34,41–56]), an approach particularly justified for weak interactions. The results concur with those obtained for the smallest $N = 1$ lattice, and the Lieb state energy is lower than the Hund state energy both for even and odd number of sites, even when long-range interaction is turned on. For $N = 1$ and $N = 2$, the Lieb state [1] corresponds to the minimum spin [this being $s_L = 0(\frac{1}{2})$ for $N = 1(2)$]; however, for $N = 3$ and $N = 4$ the paramagnetic state—of minimum spin—differs from the Lieb state and emerges as ground state when the interaction ratio (long range versus Hubbard) exceeds a certain value. This is attributed to the long-range interaction favoring the lowest spin ground state [57].

Various shape of nanoscale lattices can be created as artificial semiconductor quantum-dot molecules [58]. We briefly mention the experimental realization of quadruple quantum-dot molecules [59] and theoretical investigations related to this subject, including also the interaction effects of half-filled systems [60]. The artificial benzene molecule is theoretically studied [61] and is proposed as an ultracold atom system in Ref. [62]. Using GaAs, InAs, or Si quantum dots as building blocks, various sizes of Lieb-type systems with interdot distances $a = 5 \div 100$ nm [16] can be tailored. This opens the possibility of exploring the properties of a Hubbard-like interaction Hamiltonian in few-site Lieb lattices, as studied here.

The outline of the paper is as follows: In Sec. II we give the Hamiltonian and describe the singlet-triplet formulation, Sec. III gives both analytical insights and exact diagonalization results for the one-cell Lieb lattice, while Sec. IV addresses numerically bigger cells with $N = 2 \div 4$. The Appendixes provide calculations details for the main sections and also analytical insights on the two-cell Lieb lattice.

## II. INTERACTING HAMILTONIAN. SINGLET AND TRIPLET OPERATORS

Let us consider a 2D lattice with the noninteracting Hamiltonian $\hat{H}_0$ having the single-particle eigenstates (or noninteracting orbitals in Ref. [63]) $\Phi_\alpha$ and the corresponding energies $\epsilon_\alpha$. When the electron-electron interaction is considered as well, the total Hamiltonian can be generically written in the second quantization:

$$\hat{H} = \hat{H}_0 + \hat{H}_{\text{int}} = \sum_{\alpha,\sigma} \epsilon_\alpha c^\dagger_{\alpha\sigma} c_{\alpha\sigma} + \frac{1}{2} \sum_{\alpha,\beta,\gamma,\delta} \sum_{\sigma\sigma'} V_{\alpha\beta,\gamma\delta} c^\dagger_{\alpha\sigma} c^\dagger_{\beta\sigma'} c_{\delta\sigma'} c_{\gamma\sigma}, \quad (1)$$

where $c^\dagger_{\alpha\sigma}$ and its conjugated $c_{\alpha\sigma}$ are the fermionic creation and annihilation operators of the states $|n_{\alpha\sigma}\rangle$ in the occupation number base, corresponding to one electron in the state $\Phi_\alpha$ with spin $\sigma = \pm 1/2$. $V_{\alpha\beta,\gamma\delta}$ are the Coulombian matrix elements expressed as the scalar products

$$V_{\alpha\beta,\gamma\delta} = \langle \Phi_\alpha(1)\Phi_\beta(2)|V(1,2)|\Phi_\gamma(1)\Phi_\delta(2)\rangle, \quad (2)$$

with $V(1,2)$ the interaction potential between the particles 1 and 2 and $\Phi(1)$ or $\Phi(2)$ are eigenstates of the particle 1 or 2. The states and energies of the many-particle Hamiltonian will

be noted with $\Psi$ and $E$; the spin quantum numbers are $s$ for the total spin operator $\hat{S}$ and $m_s$ for its projection $\hat{S}_z$. The energy unit is the hopping integral that is considered $t = 1$ and we work with $\hbar = 1$.

In the tight-binding model, suitable for lattices such as the Lieb ones we consider here, the Coulombian matrix elements are the sum of on-site Hubbard and intersite long-range interaction terms [49,63]:

$$V_{\alpha\beta,\gamma\delta} = U_H \sum_i \Phi_\alpha(i)^* \Phi_\beta(i)^* \Phi_\gamma(i) \Phi_\delta(i) + V_L \sum_{i \neq j} \frac{\Phi_\alpha(i)^* \Phi_\beta(j)^* \Phi_\gamma(i) \Phi_\delta(j)}{|R_i - R_j|}, \quad (3)$$

where $i,j$ are the discrete lattice sites and $R_i, R_j$ are their space coordinates that are expressed in terms of the lattice constant $a$. In Fig. 1, $a$ is the square length. $U_H$ and $V_L$ give the Hubbard and long-range interaction strengths. For a quantum dot array with the confinement potential described in Ref. [16] the Hubbard parameter is $U_H = \frac{\sqrt{2\pi}e^2}{4\pi\epsilon d}$ with $d$ being the dot radius depending on the confinement and $\epsilon$ being the dielectric constant. If we consider the long-range interaction parameter $V_L = \frac{e^2}{4\pi\epsilon a}$ we obtain the ratio $V_L/U_H = \frac{d}{a\sqrt{2\pi}}$. As example, by varying the dot radius $0 < d < 0.2a$ the ratio $V_L/U_H$ can be modified from 0 to 0.5. We use these values in the numerical calculations.

As is well known, the Hamiltonian commutes with the spin operators $\hat{S}$ and $\hat{S}_z$. As a consequence, and as will be seen in the following sections, the eigenfunctions for two electrons will always be singlet ($s = 0, m_s = 0$) or triplet ($s = 1, m_s = 0, \pm 1$) states that are obtained by acting the following singlet and triplet operators on the vacuum:

$$\hat{S}_{\alpha\alpha} = c^\dagger_{\alpha\uparrow} c^\dagger_{\alpha\downarrow}, \quad (4)$$

$$\hat{S}_{\alpha\beta} = \frac{1}{\sqrt{2}}(c^\dagger_{\alpha\uparrow} c^\dagger_{\beta\downarrow} - c^\dagger_{\alpha\downarrow} c^\dagger_{\beta\uparrow}), \quad \text{for } \alpha \neq \beta, \quad (5)$$

$$\hat{T}^0_{\alpha\beta} = \frac{1}{\sqrt{2}}(c^\dagger_{\alpha\uparrow} c^\dagger_{\beta\downarrow} + c^\dagger_{\alpha\downarrow} c^\dagger_{\beta\uparrow}), \quad (6)$$

$$\hat{T}^{+1}_{\alpha\beta} = c^\dagger_{\alpha\uparrow} c^\dagger_{\beta\uparrow}, \quad (7)$$

$$\hat{T}^{-1}_{\alpha\beta} = c^\dagger_{\alpha\downarrow} c^\dagger_{\beta\downarrow}. \quad (8)$$

The singlet and triplet states are simply a change of basis for the operators pairs that appear in the Hamiltonian, and we can easily derive the matrix elements of $\hat{H}_{\text{int}}$ in this basis, relations that will prove useful in the following spectral calculations:

$$\langle S_{\alpha\alpha}|\hat{H}_{\text{int}}|S_{\gamma\gamma}\rangle = V_{\alpha\alpha,\gamma\gamma}, \quad (9)$$

$$\langle S_{\alpha\alpha}|\hat{H}_{\text{int}}|S_{\gamma\delta}\rangle = \sqrt{2}V_{\alpha\alpha,\gamma\delta} \quad \text{with } \gamma \neq \delta, \quad (10)$$

$$\langle S_{\alpha\beta}|\hat{H}_{\text{int}}|S_{\gamma\delta}\rangle = V_{\alpha\beta,\gamma\delta} + V_{\alpha\beta,\delta\gamma} \quad \text{with} \quad \alpha \neq \beta, \quad \gamma \neq \delta, \quad \text{and} \quad (11)$$

$$\left\langle T^{m_s}_{\alpha\beta}\middle|\hat{H}_{\text{int}}\middle|T^{m_s}_{\gamma\delta}\right\rangle = V_{\alpha\beta,\gamma\delta} - V_{\alpha\beta,\delta\gamma}. \quad (12)$$

The full eigenfunctions $\Psi$ for larger number of electrons (for the one-cell lattice for instance we shall need *eight* electrons) will be conveniently expressed by grouping pairs of electrons into singlet and triplet states.

We mention that the Greek indices $\alpha$, $\beta$, ... are for the single-particle eigenstates (or orbital states) and Latin indices $i,j$ are for the lattice sites.

## III. ONE-CELL LIEB LATTICE

Now we shall specialize the generic Hamiltonian given in the previous section, for the particular case of a square with centered sides, depicted in Fig. 1. As shall be seen, this smallest realization of a Lieb lattice already has a degenerate level in the middle of the spectrum, raising nontrivial questions like the ground-state spin at half filling or the values of the first excitation energy. The two midspectrum degenerate levels are spatially disjoint (nonoverlapping), causing a vanishing exchange interaction between two electrons occupying them and consequently a degeneracy between singlet and triplet states. We show, however, that the degeneracy is in the favor of the singlet state, that is, remaining the unique ground state when the configurations involving the rest of the spectrum are considered. We shall present analytical results—considering single-electron excitations in the second order of perturbation—and also exact diagonalization results.

### A. Single-particle states

The one-cell Lieb lattice has eight states in the single-particle spectrum as shown in Fig. 1. We shall use the notations from Ref. [15], the eight eigenstates being grouped in three branches: the states $\Phi^\pm(\vec{k})$ for wave vectors $\vec{k} = (\pi,\pi/2)$, $(\pi/2,\pi)$ and $(\pi/2,\pi/2)$ with positive (+) and negative (−) energies $\epsilon^\pm(\vec{k}) = \pm 2t[\cos^2(k_x/2) + \cos^2(k_y/2)]^{1/2}$ and two states $\Phi^0(\vec{k})$ for $\vec{k} = (\pi,\pi)$ and $(\pi/2,\pi/2)$ with zero energy $\epsilon^0(\vec{k}) = 0$. For simplicity the states are also indexed $\Phi_{1\ldots8}$ and their energies are shown in Fig. 1.

We give below the expression for the first five quantum states (vanishing boundary conditions have been implicitly assumed, meaning that the wave functions are normalized on the eight sites of the system and vanish outside, also no periodicity conditions are imposed):

$$\Phi^-_1\left(\frac{\pi}{2},\frac{\pi}{2}\right) = \frac{1}{2\sqrt{2}}(-|A_{11}\rangle + |B_{11}\rangle - |A_{21}\rangle + |C_{21}\rangle - |A_{22}\rangle + |B_{12}\rangle - |A_{12}\rangle + |C_{11}\rangle), \quad (13)$$

$$\Phi^-_2\left(\pi,\frac{\pi}{2}\right) = \frac{1}{2\sqrt{2}}(-|A_{11}\rangle + |A_{21}\rangle - \sqrt{2}|C_{21}\rangle + |A_{22}\rangle - |A_{12}\rangle + \sqrt{2}|C_{11}\rangle), \quad (14)$$

$$\Phi^-_3\left(\frac{\pi}{2},\pi\right) = \frac{1}{2\sqrt{2}}(-|A_{11}\rangle + \sqrt{2}|B_{11}\rangle - |A_{21}\rangle + |A_{22}\rangle - \sqrt{2}|B_{12}\rangle + |A_{12}\rangle), \quad (15)$$

$$\Phi^0_4(\pi,\pi) = \frac{1}{2}(|A_{11}\rangle - |A_{21}\rangle + |A_{22}\rangle - |A_{12}\rangle), \quad \text{and} \quad (16)$$

$$\Phi^0_5\left(\frac{\pi}{2},\frac{\pi}{2}\right) = \frac{1}{2}(|B_{11}\rangle - |C_{21}\rangle + |B_{12}\rangle - |C_{11}\rangle). \quad (17)$$

Some comments are in order:

(i) The states $\Phi^+(\vec{k})$ are obtained from the states $\Phi^-(\vec{k})$ changing the sign of $A$ sites' coefficients. This is an electron-hole symmetry operation that changes a state with energy $\epsilon$ in the state with energy $-\epsilon$ and changes the sign of the wave function projected on one of the sublattices [38–40]. In our case $\Phi^+(\vec{k};A) = -\Phi^-(\vec{k};A)$ and $\Phi^+(\vec{k};B,C) = \Phi^-(\vec{k};B,C)$.

(ii) In the finite Lieb lattice there is a degenerate level $\epsilon = 0$ at midspectrum having one of the degenerate states located on $A$ sites and all of the other states located on $B$ and $C$ sites [15]. For one cell the degeneracy of the zero-energy level is $g = 2$ and, following the introduced notation, $\Phi_4$ is localized on $A$ lattice sites and $\Phi_5$ on $B,C$ lattice sites, thus making them spatially disjoint. This nonoverlapping property of single-particle wave functions one has to keep in mind, as it will play an important role for the many-body spectrum, leading, for instance, to the missing of ferromagnetism in a flat band [64]. The property of certain eigenfunctions being exactly *zero* in some lattice sites was proven to be important also for building generalized eigenfunctions for bigger lattices built by so-called origami rules [65].

(iii) Our Hamiltonian has parity symmetry and consequently the eigenstates are even or odd in respect to the parity operators $\hat{P}_x$ and $\hat{P}_y$ that change $x$ in $-x$ and $y$ in $-y$, respectively. The states are even at parity operation on $x$ direction when $\hat{P}_x\Phi = \Phi$ and we say they have the property $E_x$, and the states are odd when $\hat{P}_x\Phi = -\Phi$ and they have the property $O_x$. For parity on $y$ direction we note with $E_y$ and $O_y$. The parity properties of the eigenstates are written in Fig. 1. When the electron-electron interaction is considered the parity becomes an important property because the interaction does not mix the many-particle states with different parity due to the selection rules of the Coulombians $V_{\alpha\beta,\gamma\delta}$ defined in Eq. (2). For instance, an excitation involving an electron transition from the state $\Phi_2^-$ to the state $\Phi_6^+$ is allowed but to the state $\Phi_7^+$ is forbidden.

### B. Two electrons on the degenerate zero levels

Keeping in mind that the subject of our paper regards the half-filled Lieb lattices (which for the one cell translates in placing eight electrons on the eight states), one can intuitively picture a situation at small interaction strength with the lowest energy states ($\Phi_1$, $\Phi_2$, and $\Phi_3$) double occupied and the remaining two electrons to be placed on the two degenerate states at midspectrum ($\Phi_4$ and $\Phi_5$). This situation is pictured in Fig. 3(a).

It is instructive to address first the simplified situation in which we neglect the interaction of these two topmost electrons with the lower fully occupied states, which is similar to considering an isolated flat band and places us in the frame of the Mielke theorem [24].

As the interaction conserves the spin, the Hamiltonian is block diagonal in the total spin subspace, and the two-particle eigenfunctions are the singlets and the triplets. The eigenenergies can be straightforwardly derived: $E(S_{44}) = V_{44,44}$, $E(S_{55}) = V_{55,55}$, $E(S_{45}) = V_{45,45} + V_{45,54}$, and $E(T_{45}) = V_{45,45} - V_{45,54}$ with exchange term $V_{45,54} = 0$. Using the single-particle functions Eqs. (16) and (17), one obtains the following energies:

$$E(S_{44}) = \frac{4+\sqrt{2}}{8}V_L + \frac{1}{4}U_H \simeq 0.67V_L + 0.25U_H, \quad (18)$$

$$E(S_{55}) = \frac{1+2\sqrt{2}}{4}V_L + \frac{1}{4}U_H \simeq 0.95V_L + 0.25U_H, \quad (19)$$

$$E(S_{45}) = \frac{5+\sqrt{5}}{5}V_L \simeq 1.44V_L, \quad (20)$$

$$E\left(T_{45}^{m_s}\right) = \frac{5+\sqrt{5}}{5}V_L \simeq 1.44V_L. \quad (21)$$

Let us briefly discuss the possible ordering on the real axis of the above-defined energies.

(1) For Hubbard interaction only, $U_H \neq 0$ and $V_L = 0$, the ground state has the degeneracy $g = 4$ and this corresponds to $E(S_{45}) = E(T_{45}^{m_s}) \equiv E_G = 0$.

(2) For long-range interaction only, $V_L \neq 0$ and $U_H = 0$, all energies linearly increase with $V_L$. The ground state is the singlet state $S_{44}$ with $E_G = 0.67V_L$.

(3) For both long-range and Hubbard interaction there are two cases that are seen in Fig. 2(a). (i) When $V_L < V_0$ with $V_0 \simeq 0.32U_H$ the ground state has degeneracy $g = 4$, one is the singlet state $S_{45}$ and three are the triplet states $T_{45}^{m_s}$. (ii) When $V_L > V_0$ the ground state is nondegenerate and is the singlet state $S_{44}$. The term proportional with $V_L$ in formula of $E(S_{44})$ becomes important and the singlet state $S_{44}$ will have the lowest direct energy of the long-range interaction due to its $A$ site localization (i.e., at the corners of the square).

One can easily calculate the first excitation energy (demagnetization energy, $\Delta E$) as the difference between the lowest energy of the nonmagnetic state with total spin quantum number $s = 0$ and the lowest energy of the magnetic state with spin $s = 1$, $\Delta E = E(s = 0) - E(s = 1)$. We perform this for the one-cell Lieb lattice and for octagon with the same electrostatic repulsion between nearby sites and the results are presented in Fig. 2(b). In accordance with the above discussion, one has $\Delta E = 0$ for $V_L < V_0$ and a sudden decrease of $\Delta E$ for $V_L > V_0$, with $V_0 \simeq 0.32U_H$ for one-cell Lieb lattice and $V_0 \simeq 0.36U_H$ for octagon. The same qualitative behavior of sudden decrease for $\Delta E$ at a given ratio $V_L/U_H$ is also seen in Fig. 5 where the numerical calculations are performed, however, at a lower ratio value for Lieb lattice due to the electrostatic repulsion with the electrons from the other levels (which supplementarily favor the configuration $S_{44}$ with the electrons in the corners being at maximum average distance from the rest of the charge, as shall be discussed).

For both systems, the one-cell Lieb lattice and the octagon, the calculations in this subsection show that the singlet and triplet states are degenerate for low values of the ratio $V_L/U_H$, while for high values of $V_L/U_H$, the $S_{44}$ singlet becomes the ground state (degenerated with the $S_{55}$ singlet for the octagon). In the next subsection we shall see that the singlet- and triplet-states' degeneracy at low $V_L/U_H$ is lifted in the favor of the singlet state, due to the interaction with the other electrons in the lattice.

We mention that the noninteracting eigenspectra for one-cell Lieb lattice or octagon have similar features with the Hückel model [66] for a molecule with eight identical atoms and equivalent bonds. For instance, our nonoverlapping

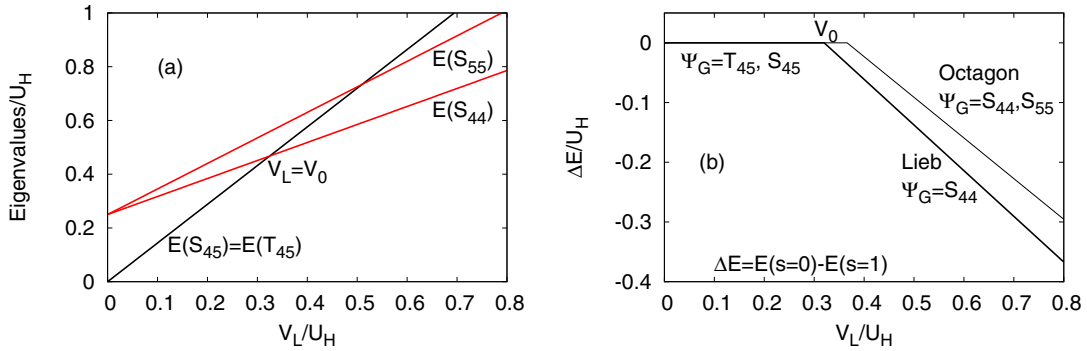


FIG. 2. (a) Energy evolution of the two-electron states $E/U_H$ from Eqs. (18)–(21) vs the ratio $V_L/U_H$ for one-cell Lieb lattice. For $V_L < V_0$ the degenerate ground state is the singlet state $S_{45}$ and the three triplets $T_{45}^{m_s}$. For $V_L > V_0$ the role of the long-range interaction increases and the nondegenerated ground state is the singlet state $S_{44}$. (b) The difference between $s = 0$ and $s = 1$ ground-state energies, $\Delta E/U_H$, vs the ratio $V_L/U_H$ for one-cell Lieb lattice and for octagon. For $V_L < V_0, \Delta E = 0$ and for $V_L > V_0, \Delta E$ decreases because a new singlet state becomes the ground state in the $s = 0$ spin sector. The features from panel (b) exhibit no Hund rule behavior. The crossing point in panel (a) and the sharp decrease of $\Delta E$ in panel (b) are for the long-range parameter value called $V_0$, that is, $V_0 \simeq 0.32U_H$ for Lieb square and $V_0 \simeq 0.36U_H$ for octagon.

zero-energy eigenstates from Eqs. (16) and (17) are the well-known nonbonding orbitals at the midspectrum of planar $D_{8h}$ cyclooctatetraene [67].

### C. First- and second-order approximations

In this subsection we want to study the lifting of the ground-state degeneracy that was seen in the previous subsection for two isolated degenerate levels if $V_L < V_0$, and for this purpose one should account for configuration mixing that implies the rest of the spectrum, by using the full eight electron wave functions.

The perturbation calculations start with considering the noninteracting ground state, corresponding to the first six electrons occupying the lowest single-particle states $\Phi_\alpha$ with $\alpha = 1,2,3$, grouped in pairs of singlets $S_{11}$, $S_{22}$, and $S_{33}$. The last two electrons occupy the degenerated states $\Phi_4$ and $\Phi_5$ with zero energy, forming pairs of triplet states $T_{45}^{m_s}$ or pairs of singlet states $S_{44}$, $S_{55}$, and $S_{45}$. In the base of the total spin operators $\hat{S}^2$ and $\hat{S}_z$ the six degenerate eigenfunctions and their parity properties are as follows:

$$\Psi_0^{m_s} = S_{11}S_{22}S_{33}T_{45}^{m_s} \quad \text{with } s = 1, \quad m_s = 0, \pm 1, \ O_x, \ O_y, \tag{22}$$

$$\Psi_0' = S_{11}S_{22}S_{33}S_{45} \quad \text{with } s = 0, \ m_s = 0, \ O_x, \ O_y, \tag{23}$$

$$\Psi_0'' = S_{11}S_{22}S_{33}S_{44} \quad \text{with } s = 0, \ m_s = 0, \ E_x, \ E_y, \tag{24}$$

$$\Psi_0''' = S_{11}S_{22}S_{33}S_{55} \quad \text{with } s = 0, \ m_s = 0, \ E_x, \ E_y. \tag{25}$$

If the interaction is turned on, the ground state will be decided between the states $\Psi_0'$ (Lieb) and $\Psi_0^{m_s}$ (Hund), since the singlets $\Psi_0''$ and $\Psi_0'''$ shall imply highest Coulomb repulsion, as seen in the simplified model of Fig. 2 for $V_L < V_0$.

One possible ground state configuration and two possible configurations obtained by single-particle transitions are shown schematically in Fig. 3 (spins are not explicitly drawn).

The spin and parity conservation rules split the total Hilbert space into subspaces, and only configurations from the same

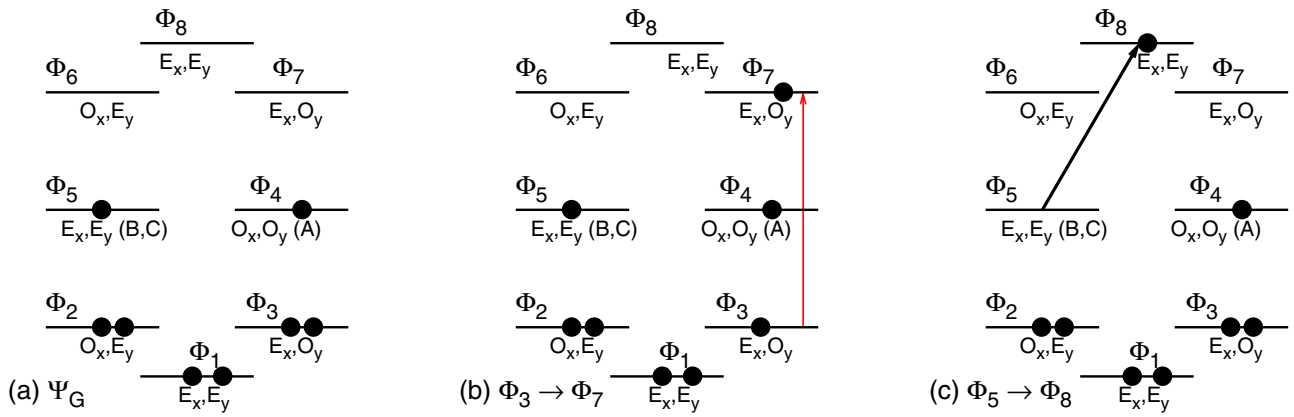


FIG. 3. The electron configuration of the noninteracting ground state (a) and of the first excited states obtained by single-particle excitation that conserve the parity of the wave functions (b, c) for one-cell Lieb lattice at half filling. The configuration in panel (b) is obtained by a symmetric transition, $\Phi_3 \to \Phi_7$, that changes the energy from $-\epsilon_{\vec{k}} \to \epsilon_{\vec{k}}$. The configuration in panel (c) is obtained by an asymmetric transition $\Phi_5 \to \Phi_8$ from a midspectrum state to an upper energy state. The single-particle states are explained in Fig. 1.

subspace can mix. Relevant subspaces for our discussion have the spin and parity properties of the four groups of noninteracting ground states above.

One can define two classes of single-electron transition processes that conserve both the spin and the parity properties: (i) First we have the symmetric transitions between states with opposite energies but the same wave vector $-\epsilon_{\vec{k}} \to \epsilon_{\vec{k}}$. In our case they are $\Phi_3 \to \Phi_7$, $\Phi_2 \to \Phi_6$, and $\Phi_1 \to \Phi_8$ with general formula of single-particle excitation energy $\Delta_{\delta,\gamma} = \epsilon_\delta - \epsilon_\gamma$. The transition $\Phi_3 \to \Phi_7$ is sketched in Fig. 3(b). As we show below, this class of transitions leads to lower energy for the singlet state. (ii) Second we have nonsymmetric transitions between one state from the flat band to a higher energy state, $\Phi_5 \to \Phi_8$, as sketched in Fig. 3(c) or opposite, from a low-energy state to the flat band, $\Phi_1 \to \Phi_5$. However, these nonsymmetric transitions contribute with identical energy shifts for both the singlet and the triplet states of the pair of flat band electrons (i.e., the states $\Psi_0'$ and $\Psi_0^{m_s}$ defined above), at least up to the second order of our perturbation calculations (not shown here, as they are technically similar with the ones given below). As such, they do not contribute to the lifting of the Lieb-Hund energy degeneracy—our main focus—and can be disregarded at this point.

We present first the calculation for the situation when the possible excited states arise from the electron transition $\Phi_3 \to \Phi_7$. If the other two symmetric transitions are considered, the second energy correction can be shown to be additive.

*(1) The ground state in the subspace with the total spin* $s = 1$ *and symmetry* $O_x, O_y$. In that case the states have $\hat{S}_z$ spin degeneracy and we consider the subspace of states with $m_s = 1$. The situation corresponds to the Hund rule with maximum spin $s_{\max} = 1$ of the two electrons on the two degenerate states $\Phi_4$ and $\Phi_5$. The nonperturbed ground state $\Psi_0$ and three possible excited states obtained by the single electron transition $\Phi_3 \to \Phi_7$ that conserve the spin and parity properties are as follows:

$$\Psi_0 = S_{11} S_{22} S_{33} T_{45}^{+1}, \tag{26}$$

$$\Psi_1 = S_{11} S_{22} T_{37}^{+1} S_{45}, \tag{27}$$

$$\Psi_2 = S_{11} S_{22} S_{37} T_{45}^{+1}, \quad \text{and} \tag{28}$$

$$\Psi_3 = \frac{1}{\sqrt{2}} S_{11} S_{22} \left( T_{37}^{0} T_{45}^{+1} - T_{37}^{+1} T_{45}^{0} \right), \tag{29}$$

with nonperturbed energies $E_0 = 2\epsilon_1 + 2\epsilon_2 + 2\epsilon_3$ and $E_1 = E_2 = E_3 = E_0 + \Delta_{7,3}$. By applying the spin operators $\hat{S}^2$ and $\hat{S}_z$ it is readily verified that $\hat{S}^2\Psi = 2\Psi$ and $\hat{S}_z\Psi = \Psi$, meaning $s = 1$ and $m_s = 1$.

The first-order energy correction is $w_{00} = \langle \Psi_0 | \hat{H}_{\text{int}} | \Psi_0 \rangle$ and the second energy correction is given by the transition amplitudes: $w_{10} = \langle \Psi_1 | \hat{H}_{\text{int}} | \Psi_0 \rangle$, $w_{20} = \langle \Psi_2 | \hat{H}_{\text{int}} | \Psi_0 \rangle$, and $w_{30} = \langle \Psi_3 | \hat{H}_{\text{int}} | \Psi_0 \rangle$. The first- and second-order corrections of the energy $E_0$ give the value

$$E(s = 1) = E_0 + w_{00} - \frac{w_{10}^2 + w_{20}^2 + w_{30}^2}{E_1 - E_0}, \tag{30}$$

with $E_1 - E_0 = \Delta_{7,3}$.

*(2) The ground state in the subspace with total spin* $s = 0, m_s = 0$ *and parity* $O_x, O_y$. This situation corresponds to the ground state spin given by the Lieb theorem that states the total spin should be $s = 0$. In this case the noninteracting ground state $\Psi_0'$ and two possible excited states $\Psi_1'$ and $\Psi_2'$ that account for the one-electron excitation process $\Phi_3 \to \Phi_7$ are as follows:

$$\Psi_0' = S_{11} S_{22} S_{33} S_{45}, \tag{31}$$

$$\Psi_1' = \frac{1}{\sqrt{3}} S_{11} S_{22} \left( T_{37}^{0} T_{45}^{0} - T_{37}^{+1} T_{45}^{-1} - T_{37}^{-1} T_{45}^{+1} \right), \quad \text{and} \tag{32}$$

$$\Psi_2' = S_{11} S_{22} S_{37} S_{45}, \tag{33}$$

with the noninteracting energies $E_0' = E_0$ and $E_1' = E_2' = E_1$, the same as in the subspace with $s = 1$. They are also eigenstates of spin operators with $\hat{S}^2\Psi = 0$ and $\hat{S}_z\Psi = 0$, meaning $s = 0$ and $m_s = 0$.

The first-order energy correction $w_{00}' = \langle \Psi_0' | \hat{H}_{\text{int}} | \Psi_0' \rangle$ and the transition amplitudes that give the second-energy corrections are $w_{10}' = \langle \Psi_1' | \hat{H}_{\text{int}} | \Psi_0' \rangle$ and $w_{20}' = \langle \Psi_2' | \hat{H}_{\text{int}} | \Psi_0' \rangle$. In the first and second orders of the perturbation theory the energy will be

$$E'(s = 0) = E_0 + w_{00}' - \frac{w'^2_{10} + w'^2_{20}}{E'_1 - E'_0}, \tag{34}$$

with $E'_1 - E'_0 = \Delta_{7,3}$.

We have derived the following useful relations for the transition amplitudes:

$$w_{00} = C + V_{45,45} - V_{45,54}, \tag{35}$$

$$w_{00}' = C + V_{45,45} + V_{45,54}, \tag{36}$$

$$w_{10}' = \sqrt{3} w_{10}, \tag{37}$$

$$w_{20}' = w_{20}, \tag{38}$$

where the energy term $C$ depends on other interaction processes except for those implying exclusively the states $\Phi_4$ and $\Phi_5$. The first energy corrections $w_{00}$ and $w_{00}'$ are different by the exchange interaction $V_{45,54}$ as the difference between the simple triplet and singlet states $T_{45}$ and $S_{45}$ that can be seen from Eqs. (11) and (12). The Eqs. (35), (36), and (38) can be shown by straightforward calculations and Eq. (37) is derived in Appendix A.

We are interested in the energy difference between the $s = 0$ and $s = 1$ spin states. Using Eqs. (30) and (34) and relations between the matrix elements, Eqs. (35)–(38), we calculate that $\Delta E = E'(s = 0) - E(s = 1)$ depends on $w_{10}, w_{30}, V_{45,54}$ and does not depend on $w_{20}$. Consequently we calculate the matrix elements $w_{10}$ and $w_{30}$, obtaining

$$w_{10} = \frac{1}{\sqrt{2}} (V_{74,43} - V_{75,53}), \tag{39}$$

$$w_{30} = V_{74,43} + V_{75,53}, \tag{40}$$

and using them we obtain the following formula for the energy difference $\Delta E$ expressed in the terms on the Coulombian

matrix elements and excitation energy $\Delta_{7,3} = \epsilon_7 - \epsilon_3$:

$$\Delta E = 2V_{45,54} + \frac{4V_{74,43}V_{75,53}}{\Delta_{7,3}}. \quad (41)$$

We note that $\Delta E$ was obtained considering the single-particle excitation $\Phi_3 \rightarrow \Phi_7$ [Fig. 3(b)]. If the other single-electron transitions ($\Phi_2 \rightarrow \Phi_6$ and $\Phi_1 \rightarrow \Phi_8$) are also considered, the energy difference becomes

$$\Delta E = 2V_{45,54} + \sum_{(\delta,\gamma)} \frac{4V_{\delta 4,4\gamma}V_{\delta 5,5\gamma}}{\Delta_{\delta,\gamma}}, \quad (42)$$

with the summation over the pairs of the states $(\delta,\gamma) = (6,2)$, $(7,3)$, and $(8,1)$.

*Comment 1.* In the first order of perturbation the singlet and triplet states are still degenerated because the exchange term $V_{45,54} = 0$. It comes from the nonoverlapping functions $\Phi_4$ and $\Phi_5$ [see Eqs. (16) and (17)].

*Comment 2.* In the second order of the perturbation and for Hubbard interaction only we have $\Delta E < 0$, meaning the degeneracy is risen and singlet state becomes the ground state. To prove this we consider the electron-hole symmetry of the states $(\gamma,\delta)$, meaning that $\Phi_\gamma(B,C) = \Phi_\delta(B,C)$ and $\Phi_\gamma(A) = -\Phi_\delta(A)$, and use the localization properties of states $\Phi_4$ and $\Phi_5$ saying that $\Phi_4(B,C) = 0$ and $\Phi_5(A) = 0$. One obtains $V_{\delta 4,4\gamma} = -V_{\delta 5,5\gamma}$ and $\Delta E < 0$.

We show the above result, performing the calculation of the interaction matrix elements in the absence of the long-range interaction. Using the eigenvectors $\Phi^-$ from Eqs. (13)–(17) and their *e-h* pairs $\Phi^+$, from Coulombian matrix Eq. (3) one obtains $V_{\delta 4,4\gamma} = -V_{\delta 5,5\gamma} = -U_H/8$ for $(\delta,\gamma) = (6,2)$, $(7,3)$, and $(8,1)$. The single-particle excitations energies are $\Delta_{6,2} = \Delta_{7,3} = 2\sqrt{2}t$ and $\Delta_{8,1} = 4t$. The energy difference becomes

$$\Delta E = -\frac{U_H^2}{16\sqrt{2}t} - \frac{U_H^2}{64t} \simeq -0.059\frac{U_H^2}{t}, \quad (43)$$

which is in good agreement with the parabolic curve obtained in the following numerical calculations of Fig. 4.

This can be regarded as an alternative proof of the Lieb theorem for the particular case of the one-loop Lieb lattice if only single-particle excitation processes are addressed at low interaction. Supplementary to that, in the low interaction limit, we have proven the missing linear term and parabolic dependence of the excitation energy on $U_H$. We notice that one obtains the same conclusions for two-cell Lieb lattice considering the same type of single-particle transitions, and the excitation energy calculation is shortly presented in Appendix B.

Numerical calculation using the formula Eq. (41) gives negative $\Delta E$ for any ratio $V_L/U_H$. Finally we remark that for interaction exceeding a crossing point $V_0$, the formula Eq. (41) no longer represents the first excitation energy, as the ground state in the $s = 0$ subspace will be the new singlet $\Psi_0''$ [Eq. (24)], thus leading to the sharp decrease of $\Delta E$ obtained in the first order of perturbation theory. This effect is explained in the previous subsection using the two-level system.

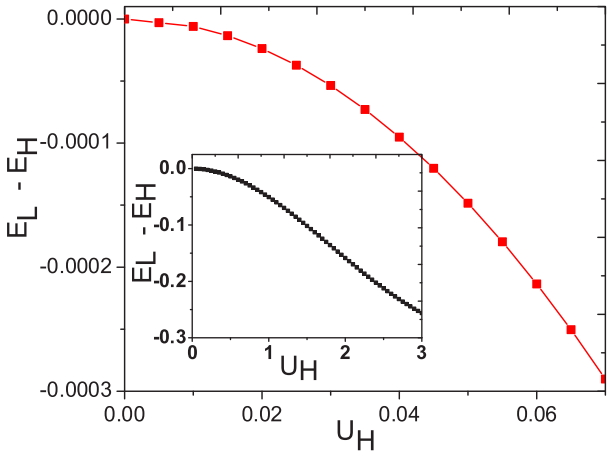


FIG. 4. Exact diagonalization results for the one-cell Lieb lattice with Hubbard interaction at half-filling. The excitation energy between the Lieb ground state (with $s = 0$) and the Hund excited state (with $s = 1$), $\Delta E = E_L - E_H$, has a parabolic dependence for small values of $U_H$ with a leading coefficient $\Delta E \simeq -0.059U_H^2$. There is a very good concordance with the perturbative analytical results from the previous subsection [see Eq. (43) for low $U_H$ values]. The inset shows that for larger values of $U_H$ the dependence becomes linear and than sublinear.

### D. Exact diagonalization

Here we present exact diagonalization results for the half-filled one-cell Lieb lattice ($N_e = 8$ electrons). This subsection is complementary to the previous ones, as it does not offer clear insights on the mechanisms involved, but on the other hand the results are numerically exact and one is not restricted to small values of the interaction strength ($U_H$ or $V_L$).

In Fig. 4 we plot the value of the inverse excitation energy $\Delta E = E(s = 0) - E(s = 1)$, i.e., the difference between the Lieb ground state energy and the excited Hund state energy, versus $U_H$. For small values of Hubbard parameter ($U_H < 1$) and zero long-range interaction, we obtain the parabolic dependence of $\Delta E$ with the value of the $U_H^2$ leading coefficient $\simeq$0.059. This is very close to the analytical one calculated in the second order of the perturbation theory in Eq. (43) for one-electron excitation processes.

For larger values of $U_H$, however, the parabolical dependence becomes linear and then sublinear, as depicted in the inset of Fig. 4. For strong interaction energies comparable or exceeding the single-particle level spacing, a very large number of configurations appear in the ground state, including those with two or more electrons on the upper energy levels (states labeled $\Phi_6$, $\Phi_7$, and $\Phi_8$ in Fig. 1). The analytical insights from Sec. III C, that are valid for weak interactions, no longer hold.

Next, we see the influence of introducing long-range interaction, an instance for which the distances between points play an important role as well. To illustrate this, we make numerical calculation for two lattice configurations that differ by the distances between their points, namely the square shape (Lieb structure) and octagon shape (which maximizes the distances between points); the results are shown in Fig. 5.

At half-filling both configurations satisfy the Lieb theorem conditions for Hubbard interaction having $s = 0$ ground state

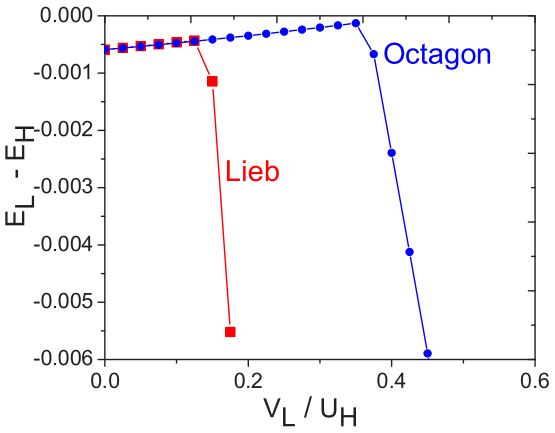


FIG. 5. The energy difference $\Delta E = E_L - E_H$ vs the ratio of the long-range vs Hubbard interactions $V_L/U_H$ for one-cell Lieb lattice and for octagon at half-filling. As the ratio $V_L/U_H$ is increased, one notices first a slight decrease in the excitation energy module (the difference $\Delta E$ slowly approaches zero), and then a sharp variation while the ground state changes to a different singlet (see description in text). The sharp decrease of $\Delta E$ happens at a long-range interaction value $V_L = V_0$ that is larger for the octagon then for the Lieb square.

spin and we want to see if it changes when the long-range interaction is present.

In Fig. 5 an interesting slight decrease for the excitation energy module, which approaches *zero*, is noticed as long-range interaction is turned on. This evolution raises the question whether one can induce a ground state spin change (by the sign change of $\Delta E$); however such an instance was not numerically found either for Lieb or for octagon configurations, which is in agreement with Eq. (42).

For larger $V_L/U_H$ ratios, one notices a sudden pronounced linear decrease of $\Delta E$ starting from a certain long-range parameter value, generically noted with $V_0$, being qualitatively similar with the curves obtained for the two-level system in Fig. 2(b). As described, this is accompanied by the changing of the ground state spatial configuration and not by the spin change.

The sharp decrease of $\Delta E$ happens at a value of the long-range parameter that is lower for the Lieb structure than for the octagon, and below we shall give insight into why this happens. For this we have a look at the singlet and triplet energy curves in Fig. 2(a) and we try to understand how they are changed when the two midspectrum electrons start to interact with the rest of the charge distribution from the occupied states $\Phi_1$, $\Phi_2$, and $\Phi_3$.

(i) In the case of a square lattice there is an energetic advantage for the midspectrum electrons to stay in the corners (on state $\Phi_4$) rather than in the middles of the sides (state $\Phi_5$ is occupied) because this maximizes the distance to the rest of the charge. The state $S_{44}$ will have a lower increase in energy compared with $S_{45}$ or $T_{45}$ and this can be seen in the difference between diagonal matrix elements of $\hat{H}_{\text{int}}$ for the states $\Psi_0$, $\Psi_0'$, and $\Psi_0''$ [see Eqs. (22), (23), and (24)]. This will lead to the decrease of the crossing point $V_0$ when the interaction with the rest of the electrons are considered. [See $V_0 \simeq 0.32U_H$ in Fig. 2(b) and $V_0 \simeq 0.14U_H$ in Fig. 5 for Lieb lattice.] (ii) This is not the case of an octagon configuration where the two states ($\Phi_4$ and $\Phi_5$) have equivalent distances to the other lattice points, being only rotated with one site. Consequently the singlet and triplet state energies increase with equal quantities when the interaction between the two midspectrum electrons and the rest of the charge is considered. It means that the crossing point $V_0$ for the octagon remains the same at least in the first order of approximation. [See $V_0 \simeq 0.36U_H$ in Figs. 2(b) and 5 for octagon.]

## IV. FEW-CELL LIEB LATTICES: NUMERICAL RESULTS

In the previous section we paid detailed attention to the one-cell Lieb lattice, taking advantage of the fact that the small number of levels allowed both for an analytical insight and for exact diagonalization at half-filling; however, this unfortunately is no longer easy or even possible for bigger lattices. Here we consider $N = 2,3$ and 4 linear cells as the one depicted in Fig. 1, meaning lattice dimensions $2\times1$, $3\times1$, and $4\times1$. The largest one would require, for instance, placing 23 electrons on 46 states for exact diagonalization, an overwhelmingly demanding computational task (equivalent to diagonalizing a matrix with the size of about $8 \times 10^{12}$).

We shall address the problem in an approximate manner, by treating the lowest electrons in a mean-field approximation and the upper ones (including the ones in the midspectrum) by the configuration-interaction approach. As in Ref. [41] the terminology refers to the situation when, even if only a certain number of single-particle levels are considered and not all (as allowed by the computing power), importantly, all the Slater determinants for a given number of electrons are then built and no truncations are performed in the Fock space. The method works for small interaction strength, when it is justified to treat the lowest occupied states in a mean-field approximation [49], as the configurations involving high-energy single-particle excitations have negligible contributions.

The $N$ linear cells Lieb lattice has $5N + 3$ single-particle states (without spin) and according to the general counting rule [37] have $N + 1$ degenerate states at midspectrum (or flat band) and $2N + 1$ states in the upper and lower bands, respectively. We shall treat the electrons on the lowest $2N + 1$ states in a mean-field approximation, meaning that the modification of the orbitals and of the eigenenergies due to electron-electron interaction is calculated using Hartree-Fock approach and these lowest electrons further influence the remaining higher ones only by the electrostatic potential created. The configuration-interaction method is then applied for the highest $N + 3$ electrons ($N + 1$ levels from the flat band plus the first level below and the first one above).

Importantly, the lattices of sizes $N = 2$ and $N = 4$ have odd numbers of total sites, which places them outside the strict conditions of the Lieb theorem, and also motivates our study to determine the ground state spin as well as the excitation energies.

The Hund state has all the electrons in the flat band with parallel spins, $s_H = s_{\max}$, meaning $s_H = (N + 1)/2$ [37]. We have $s_H = 3/2$, 2, and $5/2$ for the cells numbering $N = 2$, 3, and 4 respectively. The Lieb state corresponds to the total spin $s_L = \frac{1}{2}(N - 1)$ and we have $s_L = 1/2$, 1, and $3/2$ for $N = 2$, 3, and 4. For cells numbering $N = 3$ and $N = 4$,

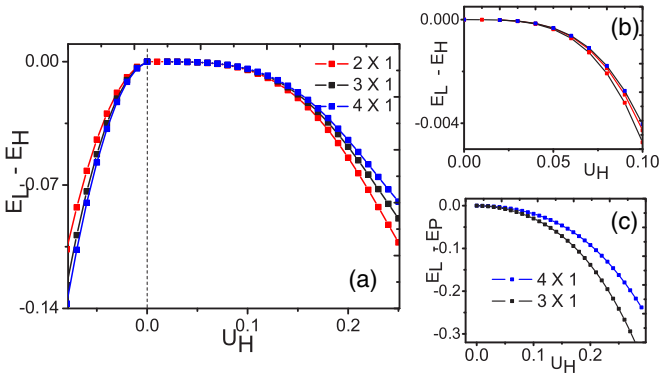


FIG. 6. (a) Difference between the Lieb and Hund energies vs $U_H$ for the Lieb lattices of sizes $2 \times 1$, $3 \times 1$, and $4 \times 1$. (b) A zoom for small $U_H$ to emphasize the parabolic behavior in this range. (c) Difference between the Lieb and paramagnetic energies, for the $3 \times 1$ and $4 \times 1$ lattices (when the two energies are distinct).

three total spin values are possible and the minimum spin for them is $s_{\min} = 0$ and $1/2$ respectively. They are referred to as paramagnetic states.

For the Hubbard interaction *only* we obtain that the Lieb state is the ground state, as for the $N = 1$ case discussed in the previous section, with the difference from the Hund energy being depicted in Fig. 6(a). Figure 6(b) is a closeup of small $U_H$, while Fig. 6(c) shows the energy difference between the Lieb and the paramagnetic states. A parabolic dependence is confirmed for small positive values of $U_H$, while for negative values of $U_H$ [Fig. 6(a)] a more abrupt, almost linear dependence is only noticed. A detailed analysis of the $U_H < 0$ regime is not intended here.

Next, we discuss the effect of turning on the long-range interaction $V_L$. We notice the abrupt change of $\Delta E = E_L - E_H$ for a given value $V_L = V_0$ in Fig. 7 for similar motifs, as discussed for the one-cell case. We mean that at $V_0$ a new state with a different spatial configuration becomes the ground state

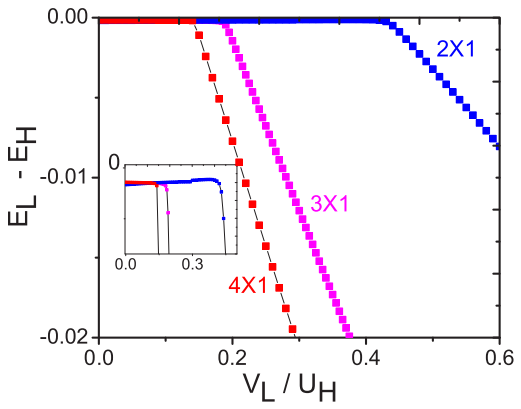


FIG. 7. Difference between the Lieb and Hund energies as long-range interaction is turned on (on the $x$ axis one has the ratio between the long-range and Hubbard interactions $V_L/U_H$), for lattices of sizes $2 \times 1$, $3 \times 1$, and $4 \times 1$. The inset shows a zoom to see that the difference is always negative, the Lieb state being the ground state. The sharp decrease of $\Delta E$ happens at a value of long range called $V_0$ that depends on the lattice size.

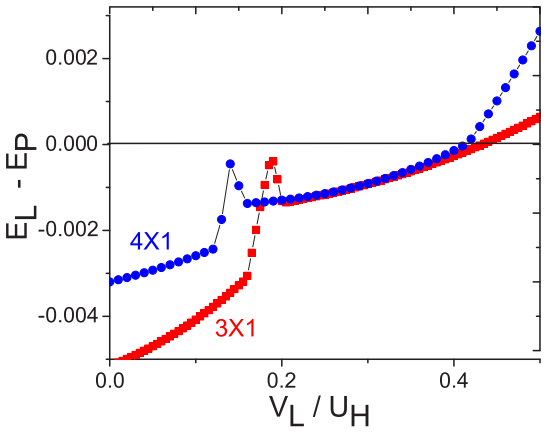


FIG. 8. Difference between the Lieb ($s_L = s_{\max} - 1$) and paramagnetic ($s_{\min} = s_{\max} - 2$) energies as function of the ratio $V_L/U_H$ for lattice sizes $3 \times 1$ and $4 \times 1$. Notice the nonmonotonic behavior (the peak for $V_L \simeq V_0$ with $V_0$ defined in Fig. 7) and the sign change (i.e., ground state spin change) for $V_L \simeq 0.4U_H$.

in the spin sector $s = s_L$. One can argue also that the long-range interaction favors the lower spin state (Lieb vs Hund).

However, for much higher long-range interaction, and if available, the third spin state with even lower spin will have the lowest energy. This is shown in Fig. 8 where the difference between the Lieb state and the paramagnetic state energies $\Delta E = E_L - E_P$ is calculated for the lattices of sizes $3 \times 1$ and $4 \times 1$.

Before the expected ground state changes into the paramagnetic one, as the ratio $V_L/U_H$ increases, one notices a nonmonotonous dependence around the value $V_L = V_0$ at which the energies in the three different spin sectors $E_H$, $E_L$, and $E_P$ are close together but not equal.

## V. SUMMARY AND CONCLUSIONS

The Lieb lattices have degenerate energy levels at midspectrum, which offer a particular instance to test the alignment of electron spins in Hund-like situations, and therefore the mechanisms involved in nanomagnetism. It is shown that the Hund state, with the maximum spin for the electrons on the degenerate levels, is not the ground state of the half-filled system, with the electrons preferring a state with one (or more) spin(s) flipped.

The electron-electron interactions, which are responsible for the nontrivial spin behavior, have been considered in this work both as on-site Hubbard term ($U_H$) and as long-range interaction ($V_L$), a case which falls outside known theorems such as Lieb [1] or Mielke [24]. Our focus was to calculate excitation energies, which are of experimental relevance.

The special attention is devoted to the smallest lattice shown in Fig. 1 for two reasons: (i) it allows analytical insights into both the second order of perturbation theory and numerical exact diagonalization for the half-filling situation and (ii) it already shows the relevant mechanisms we want to discuss. For the half-filled case, the debate is whether the two topmost electrons on the midspectrum degenerate levels are in the Hund state with total spin $s_H = s_{\max}$ equal to 1 in this case (triplet state) or in the Lieb state with $s_L = s_{\max} - 1$ (singlet state).

We emphasize the wave functions properties that *establish the Lieb state as the ground state*: (a) one of the states of the midspectrum (flat band) has no spatial overlap with the other(s) and (b) the allowed single-particle excitations take place between states related by the electron-hole symmetry [see, for instance, the transition in Fig. 3(b)]. The property b systematically leads to negative sign contributions to the level spacing $\Delta E$ between the Lieb and Hund energies, being a second-order effect of the interaction potential, while the first-order correction of $\Delta E$ is zero due to the property a. The coefficient of the parabolic dependence of $\Delta E$ on $U_H$ is calculated.

When the long-range interaction is increased and the ratio $V_L/U_H$ exceeds a certain value one obtains a *sharp variation of* $\Delta E$ with no spin change of the ground state. This is attributed to the crossing between two different singlet states in the many-particle spectrum. The ground state will change to a different singlet with two electrons occupying the state located at corners, which minimizes the Coulomb repulsion. For comparison, it is shown that such a sharp transition occurs for higher values of $V_L/U_H$ in the case of the octagon. The effect is noticed in the first order of perturbation theory and it is confirmed by exact diagonalization calculations, which address also the case of stronger interactions.

The same two properties a and b described above support the Lieb state having the minimum energy also for the two-cell Lieb lattice with Hubbard interaction, which has an odd number of lattice points, placing it outside of the Lieb theorem's strict conditions.

The numerical calculations for $N = 2 \div 4$ size lattices, using the combined mean-field plus configuration-interaction method, lead to similar results as the analytical ones, with the Lieb state being always lower in energy than the Hund state. We have again a parabolic dependence of their energy difference at small $U_H$ (and $V_L = 0$) and we obtain the sharp decrease of the excitation energy while the ratio $V_L/U_H$ exceeds a certain value (for $V_L = V_0$) that depends on the lattice size. In the Lieb lattice, there is always one of the degenerate midspectrum states that is nonoverlapping with the others [15], allowing the Lieb state to be degenerate with the Hund one for the isolated flat band and to get lower in energy when configurations involving the rest of the spectrum are taken into account.

For lattices with number of cells $N = 3$ and $N = 4$ a new state of minimum spin $s_{\min}$ has to be considered as possible ground state alongside the Hund and Lieb states. Our numerical calculations show that at small long-range interaction the Lieb state remains lower in energy, while higher values of long-range interaction promote the $s_{\min}$ state as ground state. In between there is a narrow interval for $V_L$ (around $V_L \simeq V_0$) in which the lowest energies in the three different spin sectors are very close together (but never quite equal).

The results can be experimentally realized in nanoscaled quantum dot devices, artificial molecules, or optical lattices that can be a platform for testing the quantum models as in the extended Hubbard Hamiltonian [16,58,68,69]. The interaction parameters $U_H$ and $V_L$ can be tuned, for instance, by varying the dot sizes, interdot distances, or the lattice potential.

One of the main results obtained in the paper is that the few-site Lieb lattice is an interesting example where the Hund rule of maximum spin does not apply for the midspectrum degenerate levels in the presence of Hubbard and long-range interaction as well, giving insight into the microscopic origin of this. By varying the interaction strength we obtain two regimes that differ by a strong enhancement of the Hund state excitation energy when the interacting ratio $V_L/U_H$ exceeds a certain lattice-dependent value.

## ACKNOWLEDGMENTS

We acknowledge useful discussions with A. Aldea. This work is supported by PNII-ID-PCE Research Programme (Grant No. 0091/2011) and the Core Programme Contract No. PN16-480101.

## APPENDIX A: MATRIX ELEMENTS $w_{10}$ AND $w'_{10}$

In this Appendix we want to prove Eq. (37), namely that $w'_{10} = \sqrt{3}w_{10}$. In the spin subspace with $s = 1, m_s = 1$ we consider the matrix element of $\hat{H}_{\text{int}}$,

$$w_{10} = \left\langle S_{11}S_{22}T_{37}^{+1}S_{45}\middle|\hat{H}_{\text{int}}\middle|S_{11}S_{22}S_{33}T_{45}^{+1}\right\rangle. \tag{A1}$$

In the subspace of $\hat{S}_z$ spin $m_s = 0$ (and not $s = 0$) we consider the matrix elements

$$w_1 = \left\langle S_{11}S_{22}T_{37}^{0}T_{45}^{0}\middle|\hat{H}_{\text{int}}\middle|S_{11}S_{22}S_{33}S_{45}\right\rangle, \tag{A2}$$

$$w_2 = \left\langle S_{11}S_{22}T_{37}^{+1}T_{45}^{-1}\middle|\hat{H}_{\text{int}}\middle|S_{11}S_{22}S_{33}S_{45}\right\rangle, \tag{A3}$$

$$w_3 = \left\langle S_{11}S_{22}T_{37}^{-1}T_{45}^{+1}\middle|\hat{H}_{\text{int}}\middle|S_{11}S_{22}S_{33}S_{45}\right\rangle. \tag{A4}$$

We want to show that $w_{10} = w_1 = -w_2 = -w_3$, which will help us to prove Eq. (37).

(1) By applying an $\hat{S}^-$ operator on both sides of the scalar product from definition of $w_{10}$ we obtain $w_{10} = \langle S_{11}S_{22}T_{37}^{0}S_{45}|\hat{H}_{\text{int}}|S_{11}S_{22}S_{33}T_{45}^{0}\rangle$. By writing explicitly $S_{45}$ and $T_{45}^0$ we obtain $w_{10} = w_1$. We use the fact that any scalar product of $\hat{H}_{\text{int}}$ between vectors that have more than two different occupation numbers is zero, because $\hat{H}_{\text{int}}$ is biparticle.

(2) After that we prove that $w_1 = -w_2 = -w_3$. For this we start from the expression of $w_1$ and use $T_{37}^{0}T_{45}^{0} = (-1 + \frac{1}{2}\hat{S}^+\hat{S}^-)T_{37}^{+1}T_{45}^{-1}$. Considering that the spin operators $\hat{S}^-$ and $\hat{S}^+$ commute with $\hat{H}_{\text{int}}$ and the action of $\hat{S}^-$ and $\hat{S}^+$ on any singlet pair is zero, we immediately obtain $w_1 = -w_2$.

In the same manner, using $T_{37}^{0}T_{45}^{0} = (-1 + \frac{1}{2}\hat{S}^+\hat{S}^-)$ $T_{37}^{-1}T_{45}^{+1}$ we obtain $w_1 = -w_3$.

(3) The matrix element $w'_{10}$ is $w'_{10} = \langle\Psi'_1|\hat{H}_{\text{int}}|\Psi'_0\rangle$ with $\Psi'_0$ and $\Psi'_1$ from Eqs. (31) and (32). We obtain $w'_{10}$ in the terms of $w_1, w_2, w_3$ defined above, $w'_{10} = (w_1 - w_2 - w_3)/\sqrt{3}$. Using the proved relation $w_{10} = w_1 = -w_2 = -w_3$ we immediately obtain Eq. (37): $w'_{10} = \sqrt{3}w_{10}$.

## APPENDIX B: TWO-CELL LIEB LATTICE: ANALYTICAL INSIGHTS

We consider a two-cell finite Lieb lattice ($N = 2$) as in Fig. 9. The one-electron Hamiltonian has 13 single-particle states, $\Phi_1, \ldots, \Phi_{13}$, with energies schematically depicted in Fig. 9(right). The following remarks can be made: (i) The Hamiltonian has the *e-h* symmetry specific to any bipartite lattice, with the eigenvalues being symmetric around $\epsilon = 0$. (ii)

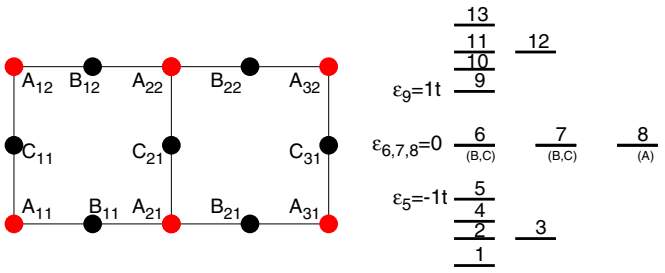


FIG. 9. (Left) The finite two-cell Lieb lattice $N = 2$ with 13 sites. The indices $n,m$ of the atoms $A$, $B$, and $C$ count the unit cells of the lattice. (Right) The single-particle eigenstates. Among them there are three states with zero energy. Two of these, $\Phi_6$ and $\Phi_7$, are localized only on $B,C$ sites, and the state $\Phi_8$ has only $A$ site localization.

The energy spectrum contains $N + 1 = 3$ zero-energy states with the known localization properties: two states localized on $B,C$ sites only ($\Phi_6$ and $\Phi_7$) and one state localized on $A$ sites ($\Phi_8$). (iii) Like the one-cell finite lattice, the two-cell lattice has also parity symmetry, which can be used as selection rule for the Coulombian matrix elements.

At half filling, for $N_e = 13$ electrons, we want to calculate the ground state spin in the second order of approximation when only one-electron excitation processes are taken into account [symmetric transitions as in Fig. 3(b)]. For the noninteracting case we consider the many-particle ground state with double occupancy for the lower energy states $\alpha = 1,\ldots,5$ while the zero-energy degenerate states $\alpha = 6,7,8$ have one electron each of them. We do not consider the state with double occupancy for $\epsilon = 0$ because, when interaction is turned on, due to Hubbard repulsion, they will have higher energy in the first-order approximation already. We work in the spin subspace with $s = m_s$. We have three noninetracting ground states, one with spin $s = 3/2$ and two states with $s = 1/2$:

$$\Psi_{\frac{3}{2}\frac{3}{2}} = S_{11}\ldots S_{55}T_{67}^{+1}n_{8\uparrow}, \tag{B1}$$

$$\Psi_{\frac{1}{2}\frac{1}{2}} = S_{11}\ldots S_{55}S_{67}n_{8\uparrow}, \tag{B2}$$

$$\Psi'_{\frac{1}{2}\frac{1}{2}} = \frac{1}{\sqrt{3}}S_{11}\ldots S_{55}\left(T_{67}^{0}n_{8\uparrow} - \sqrt{2}T_{67}^{+1}n_{8\downarrow}\right). \tag{B3}$$

The symbol $n_{8\sigma}$ means that we have one electron in the state $\Phi_8$ with spin $\sigma$. The spin properties of the states are readily verified by the actions $\hat{S}^2\Psi_{s,m_s} = s(s+1)\Psi_{s,m_s}$ and $\hat{S}_z\Psi_{s,m_s} = m_s\Psi_{s,m_s}$.

Following the same steps as for the one-cell Lieb lattice, we consider the excited states obtained by the one-electron transition $\Phi_5 \to \Phi_9$ that conserve the parity of the system and perform calculations up to the second order of approximation. We give only the principal results. (i) First we obtain that the interaction potential does not couple between the two $s = 1/2$ states, $\Psi_{\frac{1}{2}\frac{1}{2}}$ and $\Psi'_{\frac{1}{2}\frac{1}{2}}$, and the first-order lowest energy in their spin sector is for the state $\Psi'_{\frac{1}{2}\frac{1}{2}}$. These are a direct consequence of the different localization of the states $\Phi_8$ and $\Phi_7$ (or $\Phi_6$) and of the fact that the exchange energy $V_{67,76}$ is a positive quantity, at least for $V_L = 0$ [see Eq. (3)], which makes the triplet state $T_{67}^{m_s}$ have lower energy than the singlet state $S_{67}$ [see Eqs. (11) and (12)]. (ii) Second, the energy difference $\Delta E$ from the ground states with spin $s = 1/2$ and with spin $s = 3/2$ has the formula

$$\Delta E = \frac{3(V_{56,69} + V_{57,79})V_{58,89}}{\Delta_{9,5}}, \tag{B4}$$

where the first-order terms are canceled out. The excitation energy is $\Delta_{9,5} = \epsilon_9 - \epsilon_5$. Some brief comments are in order:

*Comment 1.* For Hubbard interaction ($V_L = 0$) we have negative $\Delta E$. The states $\Phi_5$ and $\Phi_9$ are related by the $e$-$h$ symmetry, meaning that $\Phi_5(A) = -\Phi_9(A)$ and $\Phi_5(B,C) = \Phi_9(B,C)$. For zero-energy states we have $\Phi_6(A) = 0, \Phi_7(A) = 0$ and $\Phi_8(B,C) = 0$. From Eq. (B4) and from Coulombian definition Eq. (3) we obtain that $V_{56,69}$ and $V_{57,79}$ are positive and $V_{58,89}$ is negative. We immediately have that $\Delta E < 0$. It means that the interacting ground state spin is $s = 1/2$, which is in agreement with the Lieb theorem result even if it is not strictly applied in our case because the two-cell Lieb lattice has an odd number of sites.

*Comment 2.* If we consider other single-particle excitation process, between states $\Phi_\gamma$ and $\Phi_\delta$ related by $e$-$h$ symmetry, formula (B4) is additive. The cancellation of the first-order corrections in the formula of energy difference is preserved and, for Hubbard interaction, $\Delta E$ remains negative in the second order of perturbation.


[1] E. H. Lieb, Phys. Rev. Lett. **62**, 1201 (1989).
[2] S. Yin, J. E. Baarsma, M. O. J. Heikkinen, J. P. Martikainen, and P. Törmä, Phys. Rev. A **92**, 053616 (2015).
[3] S. Taie, H. Ozawa, T. Ichinose, T. Nishio, S. Nakajima, and Y. Takahashi, Sci. Adv. **1**, e1500854 (2015).
[4] V. Apaja, M. Hyrkas, and M. Manninen, Phys. Rev. A **82**, 041402(R) (2010).
[5] R. Shen, L. B. Shao, B. Wang, and D. Y. Xing, Phys. Rev. B **81**, 041410(R) (2010).
[6] S. Mukherjee, A. Spracklen, D. Choudhury, N. Goldman, P. Öhberg, E. Andersson, and R. R. Thomson, Phys. Rev. Lett. **114**, 245504 (2015).
[7] R. A. Vicencio, C. Cantillano, L. Morales-Inostroza, B. Real, C. Mejía-Cortés, S. Weimann, A. Szameit, and M. I. Molina, Phys. Rev. Lett. **114**, 245503 (2015).
[8] H. Wang, S. Yu, and J. X. Li, Phys. Lett. A **378**, 3360 (2014).
[9] V. I. Iglovikov, F. Hebert, B. Gremaud, G. G. Batrouni, and R. T. Scalettar, Phys. Rev. B **90**, 094506 (2014).
[10] N. Goldman, D. F. Urban, and D. Bercioux, Phys. Rev. A **83**, 063601 (2011).
[11] C. Weeks and M. Franz, Phys. Rev. B **82**, 085310 (2010).
[12] W. F. Tsai, C. Fang, H. Yao, and J. Hu, New J. Phys. **17**, 055016 (2015).

[13] G. Palumbo and K. Meichanetzidis, Phys. Rev. B **92**, 235106 (2015).

[14] B. Jaworowski, A. Manolescu, and P. Potasz, Phys. Rev. B **92**, 245119 (2015).

[15] M. Niţă, B. Ostahie, and A. Aldea, Phys. Rev. B **87**, 125428 (2013).

[16] H. Tamura, K. Shiraishi, T. Kimura, and H. Takayanagi, Phys. Rev. B **65**, 085324 (2002).

[17] A. Zhao and S.-Q. Shen, Phys. Rev. B **85**, 085209 (2012).

[18] C. Ke-Ji and Z. Wei, Chin. Phys. Lett. **31**, 110303 (2014).

[19] J. D. Gouveia and R. G. Dias, J. Magn. Magn. Mater. **382**, 312 (2015).

[20] J. D. Gouveia and R. G. Dias, J. Magn. Magn. Mater. **405**, 292 (2016).

[21] X. Cao, K. Chen, and D. He, J. Phys.: Condens. Matter **27**, 166003 (2015).

[22] K. Noda, A. Koga, N. Kawakami, and T. Pruschke, Phys. Rev. A **80**, 063622 (2009).

[23] K. Noda, K. Inaba, and M. Yamashita, Phys. Rev. A **90**, 043624 (2014); **91**, 063610 (2015).

[24] A. Mielke, Phys. Lett. A **174**, 443 (1993); **82**, 4312 (1999).

[25] H. Tasaki, Progr. Th. Phys. **99**, 489 (1998).

[26] O. Derzhko, J. Richter, and M. Maksymenko, Int. J. Mod. Phys. B **29**, 1530007 (2015).

[27] O. Steffens, U. Rössler, and M. Suhrke, Europhys. Lett. **42**, 529 (1998).

[28] B. Partoens and F. M. Peeters, Phys. Rev. Lett. **84**, 4433 (2000).

[29] A. F. Ho, Phys. Rev. A **73**, 061601(R) (2006).

[30] M. Korkusinski, I. P. Gimenez, P. Hawrylak, L. Gaudreau, S. A. Studenikin, and A. S. Sachrajda, Phys. Rev. B **75**, 115301 (2007).

[31] K. Kärkkäinen, M. Borgh, M. Manninen, and S. M. Reimann, New J. Phys. **9**, 33 (2007).

[32] T. Sako, J. Paldus, and G. H. F. Diercksen, Phys. Rev. A **81**, 022501 (2010).

[33] S. Florens, A. Freyn, N. Roch, W. Wernsdorfer, F. Balestro, P. Roura-Bas, and A. A. Aligia, J. Phys.: Condens. Matter **23**, 243202 (2011).

[34] W. Sheng, M. Sun, and A. Zhou, Phys. Rev. B **88**, 085432 (2013).

[35] S. Schröter, H. Friedrich, and J. Madroñero, Phys. Rev. A **87**, 042507 (2013).

[36] W. T. Borden, H. Iwamura, and J. A. Berson, Acc. Chem. Res. **27**, 109 (1994).

[37] For a finite Lieb lattice with $N$ cells and vanishing boundary conditions, the degeneracy of the midspectrum level is $g = N + 1$, that is equal to $||A| - |B|| + 2$. The maximum spin at half-filing is $s_H = (N + 1)/2$. The Lieb value corresponds to one spin flipped $s_L = ||A| - |B||/2 = (N - 1)/2$. In Fig. 1 the B sublattice is labeled both with B and C to keep the notations in Ref. [15] for the elementary cell.

[38] H. Y. Deng and K. Wakabayashi, Phys. Rev. B **90**, 115413 (2014).

[39] M. Niţă, M. Ţolea, and B. Ostahie, Phys. Status Solidi RRL **08**, 790 (2014).

[40] B. Ostahie and A. Aldea, Phys. Rev. B **93**, 075408 (2016).

[41] M. Rontani, C. Cavazzoni, D. Bellucci, and G. Goldoni, J. Chem. Phys. **124**, 124102 (2006).

[42] V. Popsueva, R. Nepstad, T. Birkeland, M. Forre, J. P. Hansen, E. Lindroth, and E. Walterson, Phys. Rev. B **76**, 035303 (2007).

[43] E. Nielsen, R. P. Muller, and M. S. Carroll, Phys. Rev. B **85**, 035319 (2012).

[44] M. P. Nowak, B. Szafran, and F. M. Peeters, J. Phys.: Condens. Matter **20**, 395225 (2008).

[45] S. Schulz, S. Schumacher, and G. Czycholl, Phys. Rev. B **73**, 245327 (2006).

[46] M. Ishizuki, H. Takemiya, T. Okunishi, K. Takeda, and K. Kusakabe, Phys. Rev. B **85**, 155316 (2012).

[47] C. Daday, A. Manolescu, D. C. Marinescu, and V. Gudmundsson, Phys. Rev. B **84**, 115311 (2011).

[48] V. Moldoveanu, A. Manolescu, C. S. Tang, and V. Gudmundsson, Phys. Rev. B **81**, 155442 (2010).

[49] P. Potasz, A. D. Güçlü, A. Wojs, and P. Hawrylak, Phys. Rev. B **85**, 075431 (2012).

[50] B. Szafran, M. P. Nowak, E. Wach, and D. P. Żebrowski, Phys. Lett. A **378**, 1036 (2014).

[51] D. Mourad and G. Czycholl, Eur. Phys. J. B **78**, 497 (2010).

[52] A. Odriazola, M. M. Ervasti, I. Makkonen, A. Delgado, A. González, E. Räsänen, and A. Harju, J. Phys.: Condens. Matter **25**, 505504 (2013).

[53] D. Toroz, M. Rontani, and S. Corni, Phys. Rev. Lett. **110**, 018305 (2013).

[54] I. G. Ryabinkin and V. N. Staroverov, Phys. Rev. A **81**, 032509 (2010).

[55] F. Ţolea and M. Ţolea, Phys. B: Condens. Matter **458**, 85 (2015).

[56] K. Ferhat and A. Ralko, Phys. Rev. B **89**, 155141 (2014).

[57] E. Lieb and D. Mattis, Phys. Rev. **125**, 164 (1962).

[58] J. Wu and Z. M. Wang, *Quantum Dot Molecules*, Lecture Notes in Nanoscale Science and Technology (Springer, New York, 2013).

[59] R. Thalineau, S. Hermelin, A. D. Wieck, C. Bauerle, L. Saminadayar, and T. Meunier, Appl. Phys. Lett. **101**, 103102 (2012); M. D. Shulman, O. E. Dial, S. P. Harvey, H. Bluhm, V. Umansky, and A. Yacoby, Science **336**, 202 (2012).

[60] I. Ozfidan, A. H. Trojnar, M. Korkusinski, and P. Hawrylak, Solid State Commun. **172**, 15 (2013); C. Schilling, Phys. Rev. B **92**, 155149 (2015).

[61] G. Begemann, S. Koller, M. Grifoni, and J. Paaske, Phys. Rev. B **82**, 045316 (2010); I. Ozfidan, M. Vladisavljevic, M. Korkusinski, and P. Hawrylak, *ibid.* **92**, 245304 (2015).

[62] D.-S. Lühmann, C. Weitenberg, and K. Sengstock, Phys. Rev. X **5**, 031016 (2015).

[63] G. Benenti, G. Caldara, and D. L. Shepelyansky, Phys. Rev. Lett. **86**, 5333 (2001).

[64] P. Müller, J. Richter, and O. Derzhko, Phys. Rev. B **93**, 144418 (2016).

[65] R. G. Dias and J. D. Gouveia, Sci. Rep. **5**, 16852 (2015).

[66] E. Hückel, Z. Phys. **70**, 204 (1931); **72**, 310 (1931); **76**, 628 (1932); **83**, 632 (1933).

[67] C. Trindle and T. Wolfskill, J. Org. Chem. **56**, 5426 (1991); T. Nishinaga, T. Ohmae, and M. Iyoda, Symmetry **2**, 76 (2010).

[68] R. Walters, G. Cotugno, T. H. Johnson, S. R. Clark, and D. Jaksch, Phys. Rev. A **87**, 043613 (2013).

[69] Y. Chougale and R. Nath, J. Phys. B: At. Mol. Opt. Phys. **49**, 144005 (2016).